JCSDA Seminar
February 24, 2010

Assimilation of Space-Borne GPS Radio Occultation Data in NWP

Xiaolei Zou
Department of Meteorology
Florida State University
zou@fsu.edu

Outline

Part I: Data

(1) Introduction to GPS RO Techniques

(2) Data Processing Chain & Error Sources

Part II: Assimilation

(3) Choices for GPS RO Data Assimilation

(4) Highlights of Assimilation Results

Part III: Data Application

(5) Comparison with Large-Scale Analyses in Cloudy and Clear-Sky Conditions

(6) Cloudy Retrieval of GPS RO Data

Future Plan

Collaborators

- **My Ph. D. students & Postdoctoral fellow:**

  H. Shao, L. Lin

  F. Vandenberghe, B. Wang, H. Liu, Z. Zeng

- **Ray-tracing model:**

  S. Sokolovskii, M. Gorbunov

- **Non-local refractivity observation operator:**

  G. Hajj

- **GPS RO data:**

  R. Anthes, Y.-H. Kuo, M. Exner, D. Hunt, R. Ware,
  C. Rocken, W. Schreiner, D. Feng, B. Herman

(1) Introduction to GPS RO Techniques

What Is Measured by GPS RO Technique?

- A GPS receiver onboard an LEO satellite measures the propagation delay of the radio signals at two L-band frequencies (f_1=1.57542 GHz and f_2=1.22760 GHz) that are transmitted from a GPS satellite

- The propagation delay depends on the distribution of atmospheric refractivity as well as on the ionosphere electron density

- The ionosphere effect can be removed by combining the two propagation delays

- The wavelengths of the GPS signals are about 20 cm, at which there is very little effect of aerosols, clouds, and rain

Ray Paths

In a vacuum, radio signals travel along straight lines connecting an occulting GPS satellite and LEO satellite.

In real atmosphere, any ray path from GPS to LEO satellite is bended in the ionosphere and the atmosphere. The total bending (e.g., bending angle) can be derived given the precise positions and velocities of both satellites.

Vertical Profiles

Due to the satellite motions, the whole atmosphere from top to surface has rays passing through it, obtaining a vertical profile of bending angles from every occurrence of radio occultation.

In the lowest ~100 km of the atmosphere, the LEO satellite collects data with a 50 Hz sampling rate, resulting in ~3000 measurements in a vertical profile and a vertical resolution of about 1.5 km in the stratosphere and higher resolution of less than 0.5 km in the lower troposphere. Such an occultation takes about 1 minute.

Global Coverage □

There are 24 GPS satellites ((about 20,200 km altitude)in six orbital planes which continuously transmit electro-magnetic waves at two L-band frequencies (f_1=1.57542 GHz and f_2=1.22760 GHz).

With 24 GPS satellites, a single GPS receiver in a near-polar orbit at 800 km will observed over 500 ROs per day, which are distributed fairly uniformly about the globe.

Bending Angle of a Ray Path

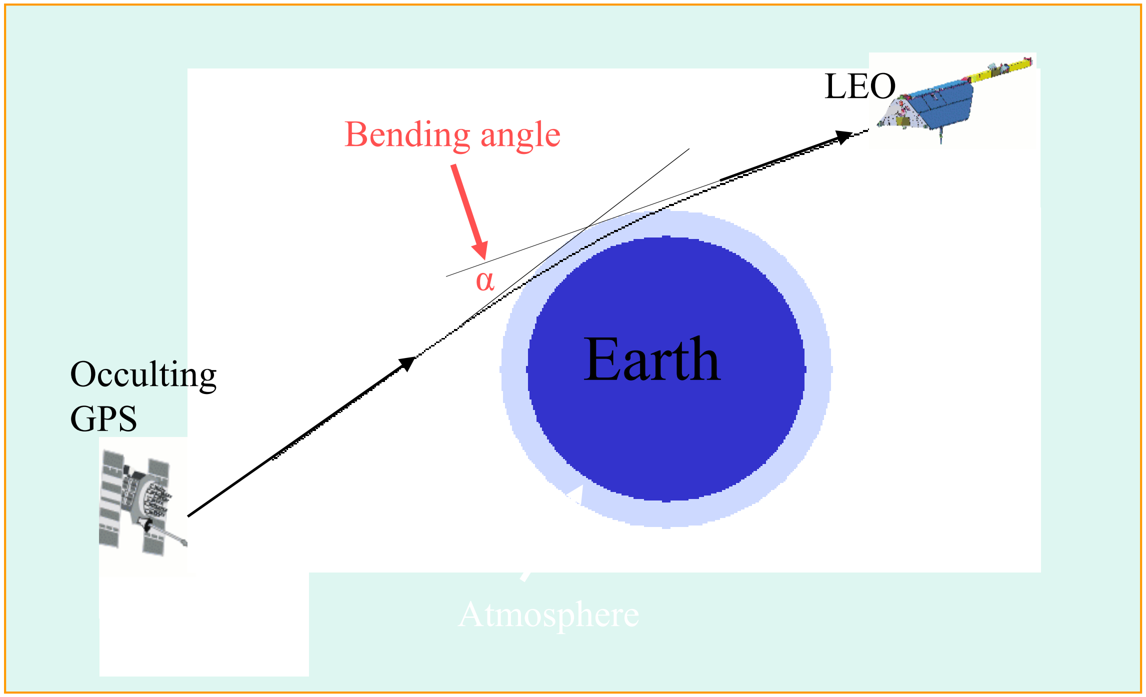

Vertical Profiling

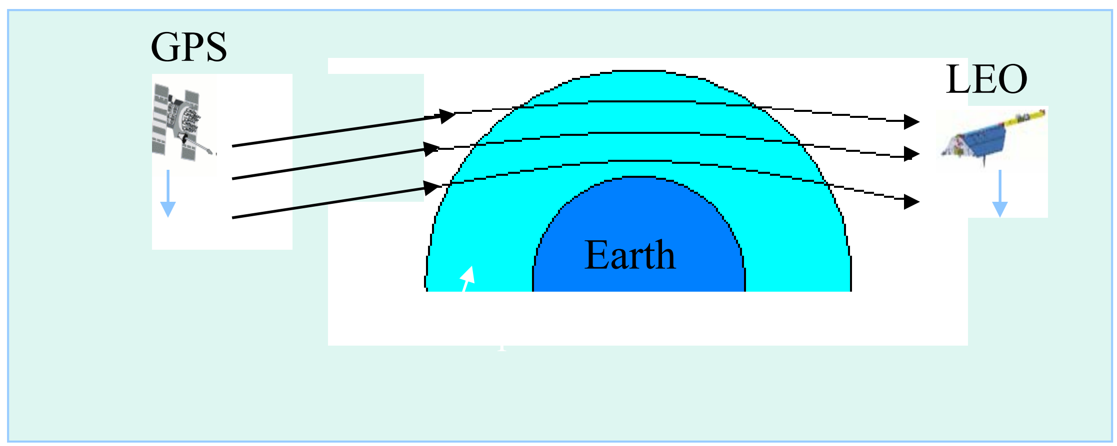

A History of GPS RO Missions

1 LEO | **1 LEO** | **1 LEO** | **6 LEOs** | **6~12 LEOs**

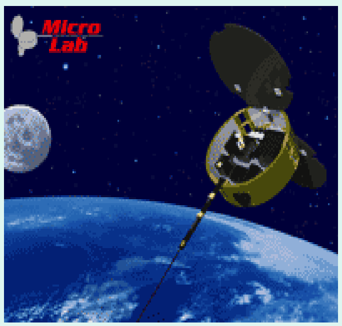

GPS/MET

CHAMP

SAC-C

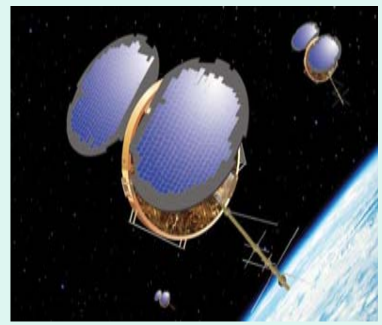

COSMIC

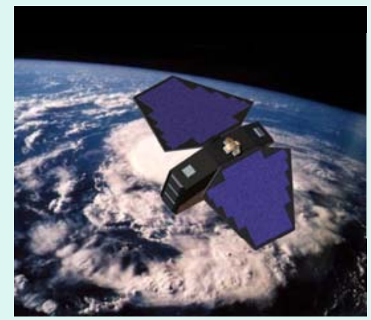

COSMIC II

April 1995 ⇨ Feb. 1997

April 2000 ⇨ present

Nov. 2000 ⇨ present

April 2006 ⇨ present

2011 ⇨

A Vertical RO Profile from CHAMP

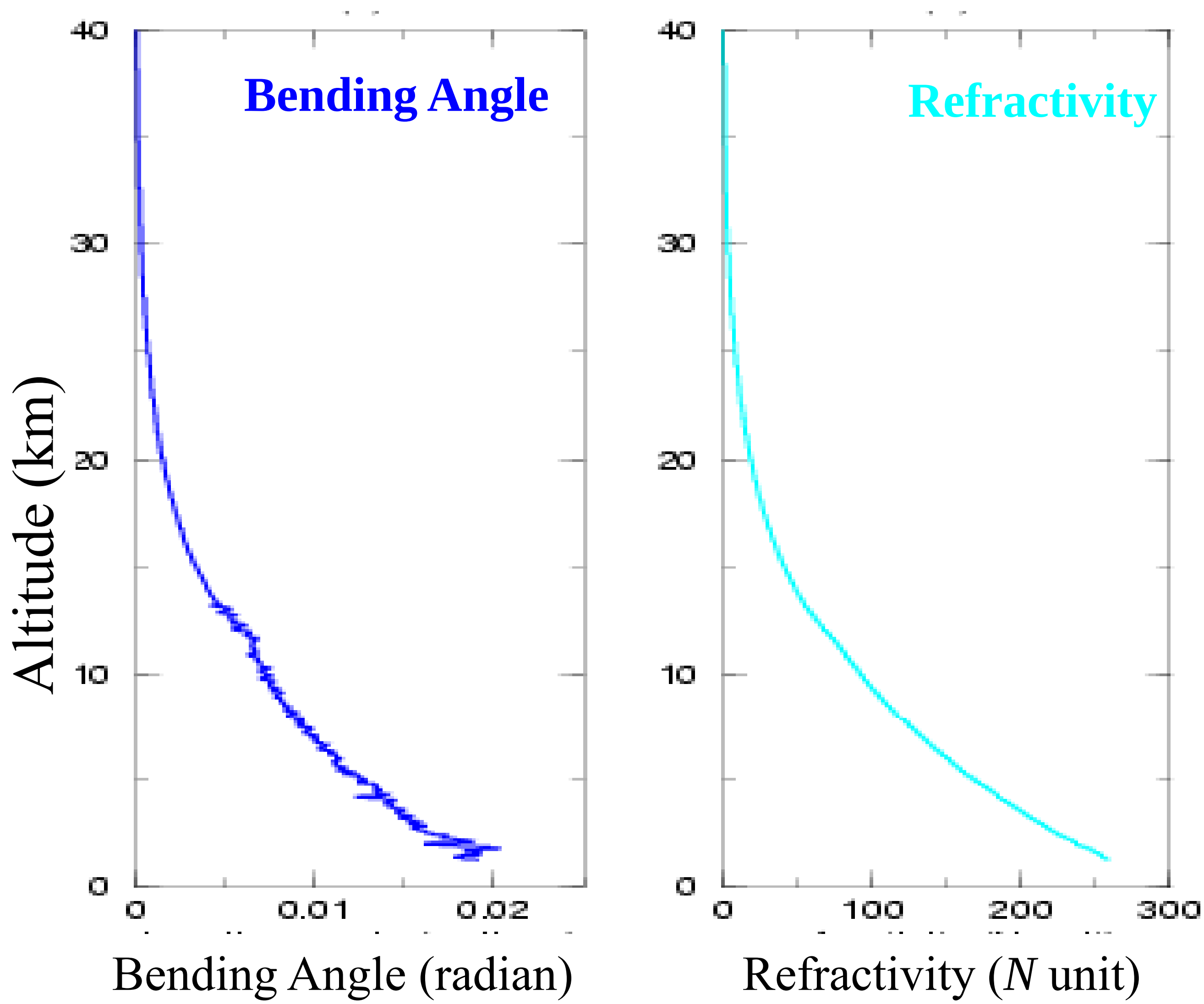

Measurement Time:

0836UTC 21 May 2002

Averaged Location:

(102.04°W, 63.40°S)

A Vertical RO Profile from CHAMP (cont.)

Locations of the tangent points

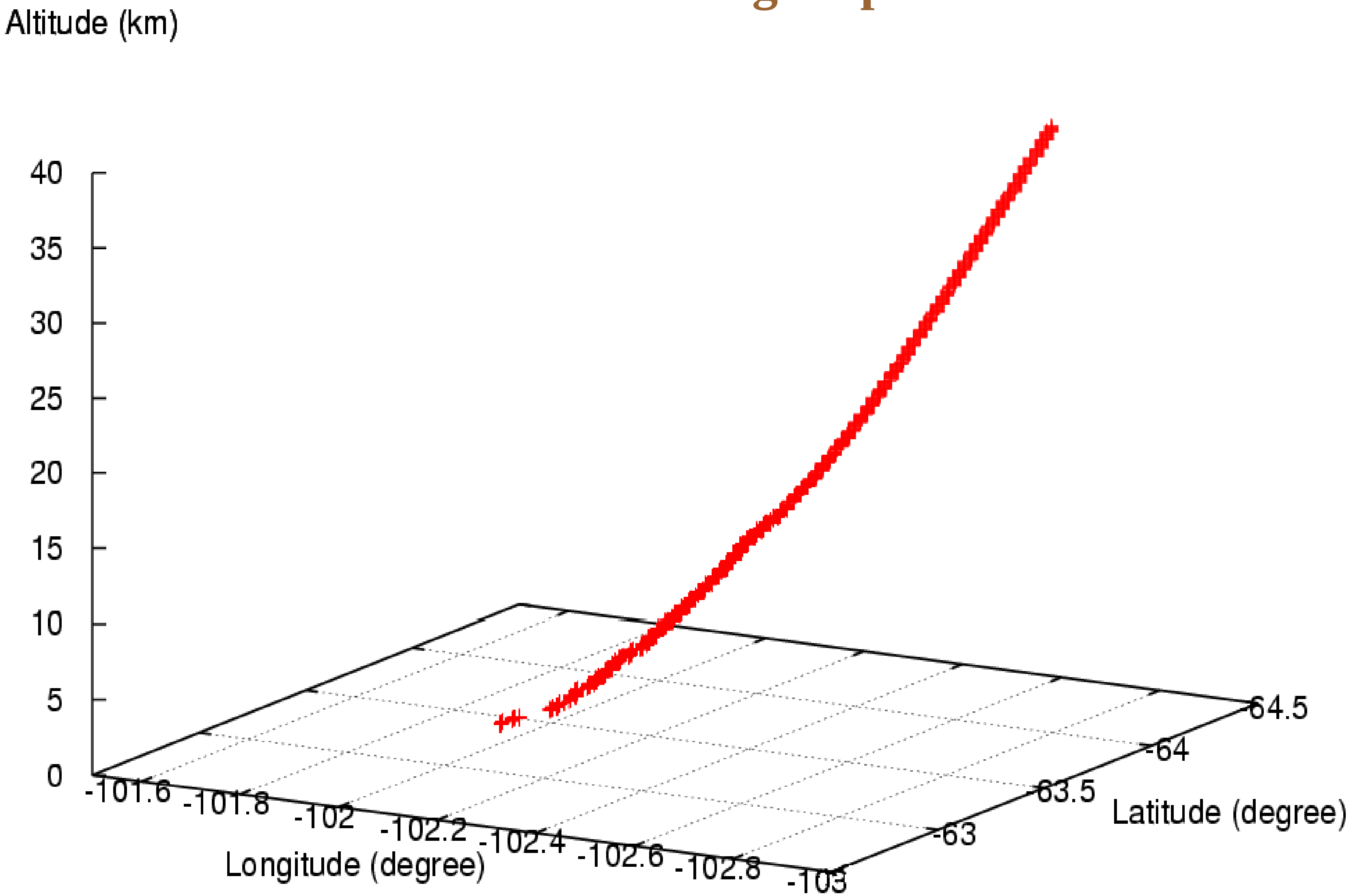

COSMIC Global Coverage on March 25, 2009

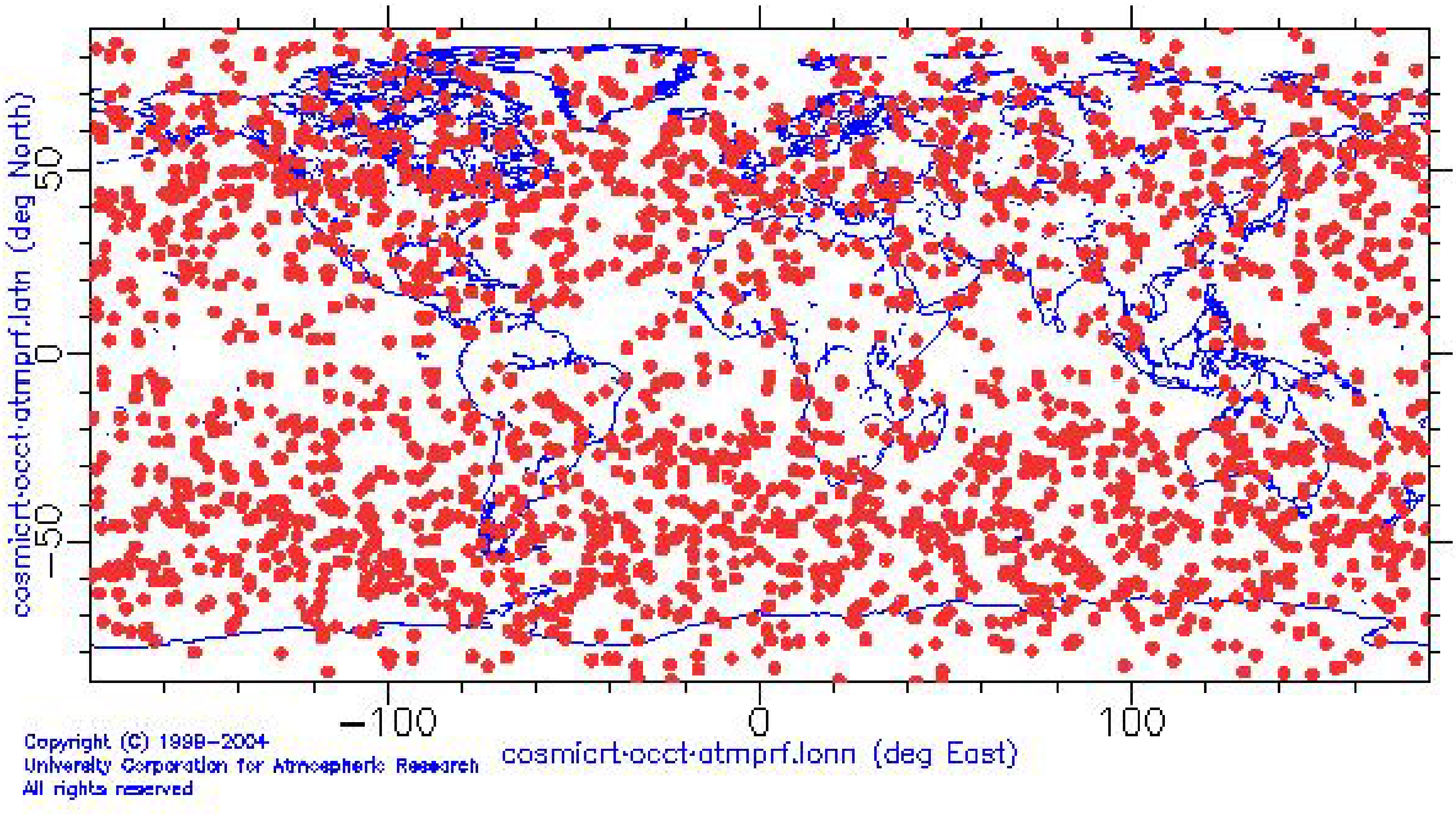

(2) Data Processing Chain & Error Sources

Data Processing Chain

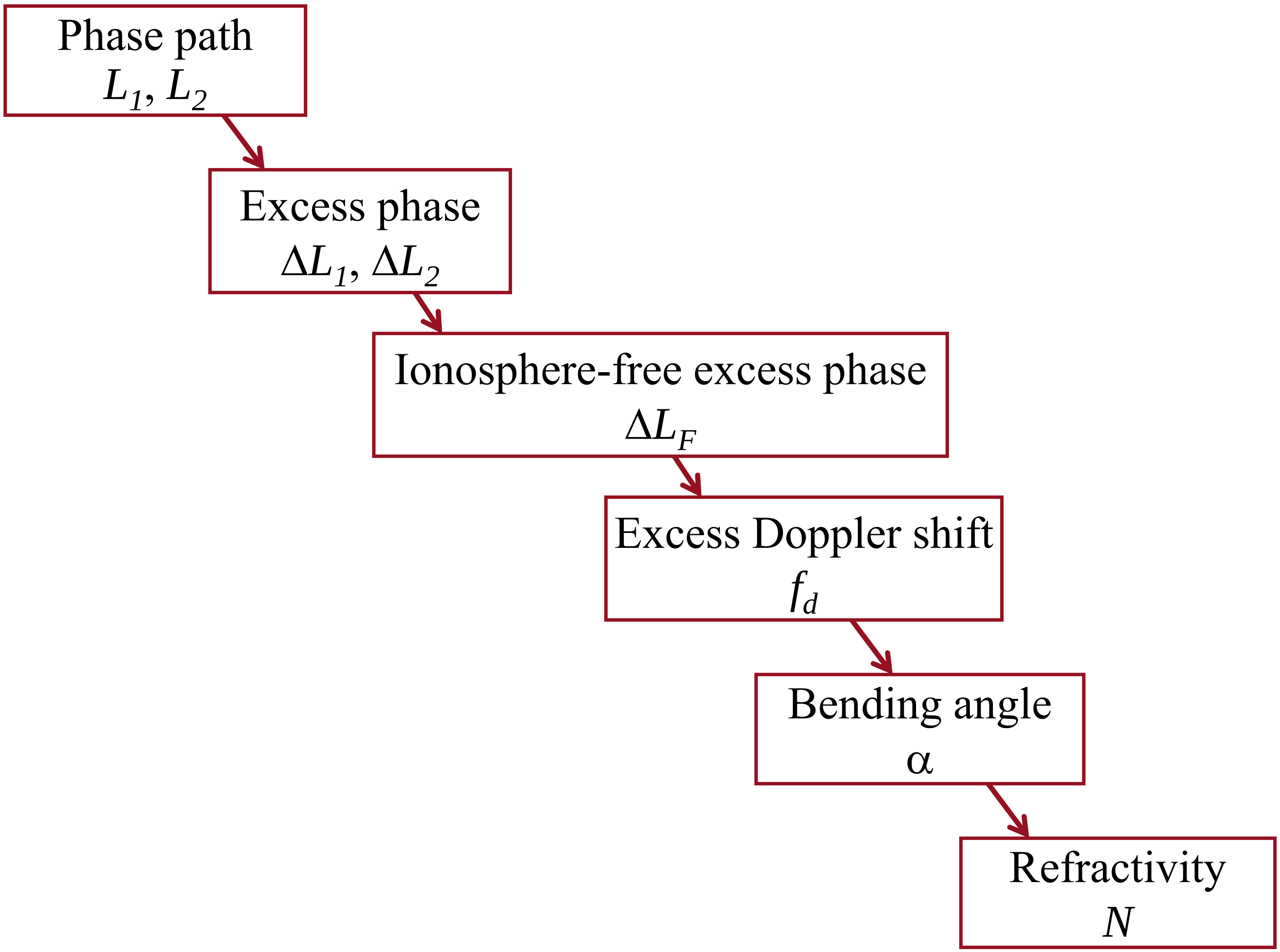

(1) Phase Path

The GPS RO observable is the phase path:

$$L_1 = \int_{GPS}^{LEO} n(f_1)ds, \qquad L_2 = \int_{GPS}^{LEO} n(f_2)ds$$

where n is the refractive index:

$$n(f) = 10^{-6}\left(k_1\frac{p_d}{T} + k_2\frac{p_w}{T} + k_3\frac{p_w}{T^2} - C\frac{N_e}{f^2}\right) + 1$$

N, contribution from the neutral atmosphere ↑   ionosphere contribution ↑

refractivity → N

(2) Excess Phase

The excess phase is calculated as the difference between the measured phase path and the "vacuum" phase path (equal to the geometric distance between GPS and LEO):

$$\Delta L_1 = L_1 - R_{GL}, \qquad \Delta L_2 = L_2 - R_{GL}$$

where R_{GL} is the geometric distance between GPS and LEO.

Signs of Refractive Index and Excess Phase

For microwave frequencies,

$n < 1$ in the ionosphere and is frequency dependent.

$n > 1$ in the neutral atmosphere and is independent of frequency.

For rays with tangent heights above the tropopause, the excess phase is negative (about 10-100 m) due to the penetration of ionospheric layers on both sides of the neutral atmosphere.

The excess phase becomes positive below the tropopause because the effect from the neutral part of the atmosphere exceeds that of the ionosphere. The excessive phase is on the order of 1 km close to the surface.

(3) Removing the Ionosphere Effect

Since the first-order contribution of the ionosphere refractivity is inversely proportional to the frequency squared, and can thus be eliminated by applying a linear combination of L1 and L2 at the same time samples:

$$L_F = \frac{f_1^2 L_1 - f_2^2 L_2}{f_1^2 - f_2^2}, \qquad \Delta L_F = \frac{f_1^2 \Delta L_1 - f_2^2 \Delta L_2}{f_1^2 - f_2^2}$$

where L_F and ΔL_F is the ionosphere free phase path and excess phase, respectively.

Magnitude of Excess Phase

The ionosphere corrected excess phase, ΔL_F is what would be measured had there been no ionosphere at all. Therefore, the ionosphere free excess phase is always positive, and is very small at the high altitude end. In fact,

$$\Delta L_F \approx \begin{cases} \text{1 mm at 80 km} \\ \text{1-9 cm at 60 km} \\ \text{1 km at the surface} \end{cases}$$

The 1-mm excess phase is less than data noise level.

(4) Excess Doppler Shift

The excess Doppler shift is derived as the time derivative of the excess phase:

$$f_d = -fc^{-1}\frac{d\Delta L}{dt}$$

where c is the light velocity in a vacuum.

(5) Bending Angle

The excess Doppler shift is related to the satellites geometry:

$$f_d = f\left(\frac{c - n_{LEO}\left(v^r_{LEO}\cos\phi_{LEO} - v^t_{LEO}\sin\phi_{LEO}\right)}{c - n_{GPS}\left(v^r_{GPS}\cos\phi_{GPS} - v^t_{GPS}\sin\phi_{GPS}\right)} - 1\right)$$

Assuming spherical symmetry:

$$\underbrace{r_{GPS}\, n_{GPS}\sin\phi_{GPS}}_{a_{GPS}} = \underbrace{r_{LEO}\, n_{LEO}\sin\phi_{LEO}}_{a_{LEO}}$$

ϕ_{LEO} (ϕ_{GPS}) is the angle between LEO (GPS) satellite radius and the tangent direction of the LEO (GPS) satellite velocity in the ray plane.

(5) Bending Angle (cont.)

Bending angle:

$$\alpha(a) = \phi_{GPS} + \phi_{LEO} + \arccos\left(\frac{\mathbf{r}_{GPS} \cdot \mathbf{r}_{LEO}}{r_{GPS} r_{LEO}}\right) - \pi$$

Impact parameter:

$$a = r_{GPS} n_{GPS} \sin \phi_{GPS}$$

(6) Refractive Index

The Abel inversion:

$$n(a) = EXP\left(\frac{1}{\pi}\int_a^\infty \frac{\alpha(x)}{\sqrt{x^2 - a^2}}dx\right),$$

(7) Refractivity

$$N = 10^6(n-1)$$

Error Sources

- **Measurement Errors:**

  (i) Random errors: Clock error and thermal noise

  (ii) Systematic errors: Signal scattering in the vicinity of the antenna, position errors, velocity errors, and retrieval errors

Retrieval errors:

(1) Ionosphere calibration errors
(2) Upper altitude boundary errors
(3) Errors introduced by the spherical symmetry assumption
(4) Errors induced by atmospheric multi-path propagation

(3) Choices for GPS RO Data Assimilation

What to Assimilate?

1. **Excess phase:** caused by the bending of the radio signal at two frequencies: *1227.6 MHz, 1575.4 MHz.*
2. **Excess Doppler frequency shift:** estimated by the time derivative of excess phase.
3. **Bending angle and impact parameter:** derived from Doppler frequency shift based on satellite geometry (impact parameter is assumed constant at GPS and LEO).
4. **Refractivity:** calculated from bending angle through the Abel inversion (the refractivity is assumed spherically symmetric).
5. **Temperature and pressure:** retrieved from refractivity using the hydrostatic equation and neglecting water vapor content.

Pros and Cons

Obs. Variable	Obs. Error Statistics	*H* *Complexity*	*H* *Comput. Cost*	Assumption(s)
ΔL^{obs}	simplest	most complex	most expensive	no SSA
α^{obs}	simple	complex	expensive	no SSA
N^{obs}	very complex	simple (N^{loc})	inexpensive	SSA
T^{obs}, q^{obs}	*most complex*	simplest	Least expensive	SSA, auxiliary info.
$\Delta L^{\text{“}obs\text{”}}$	simple	simple	inexpensive	No SSA
N^{obs}	simple	simple ($N^{non\text{-}loc}$)	inexpensive	No SSA

SSA --- Spheric Symmetry Assumption

(4) Highlights of Assimilation Results

(4a) Comparison between bending angle and refractivity assimilation

(4b) Comparison between local and non-local refractivity assimilation

Observation Operator for *N*

$$F_I H_N(T, p, q)$$

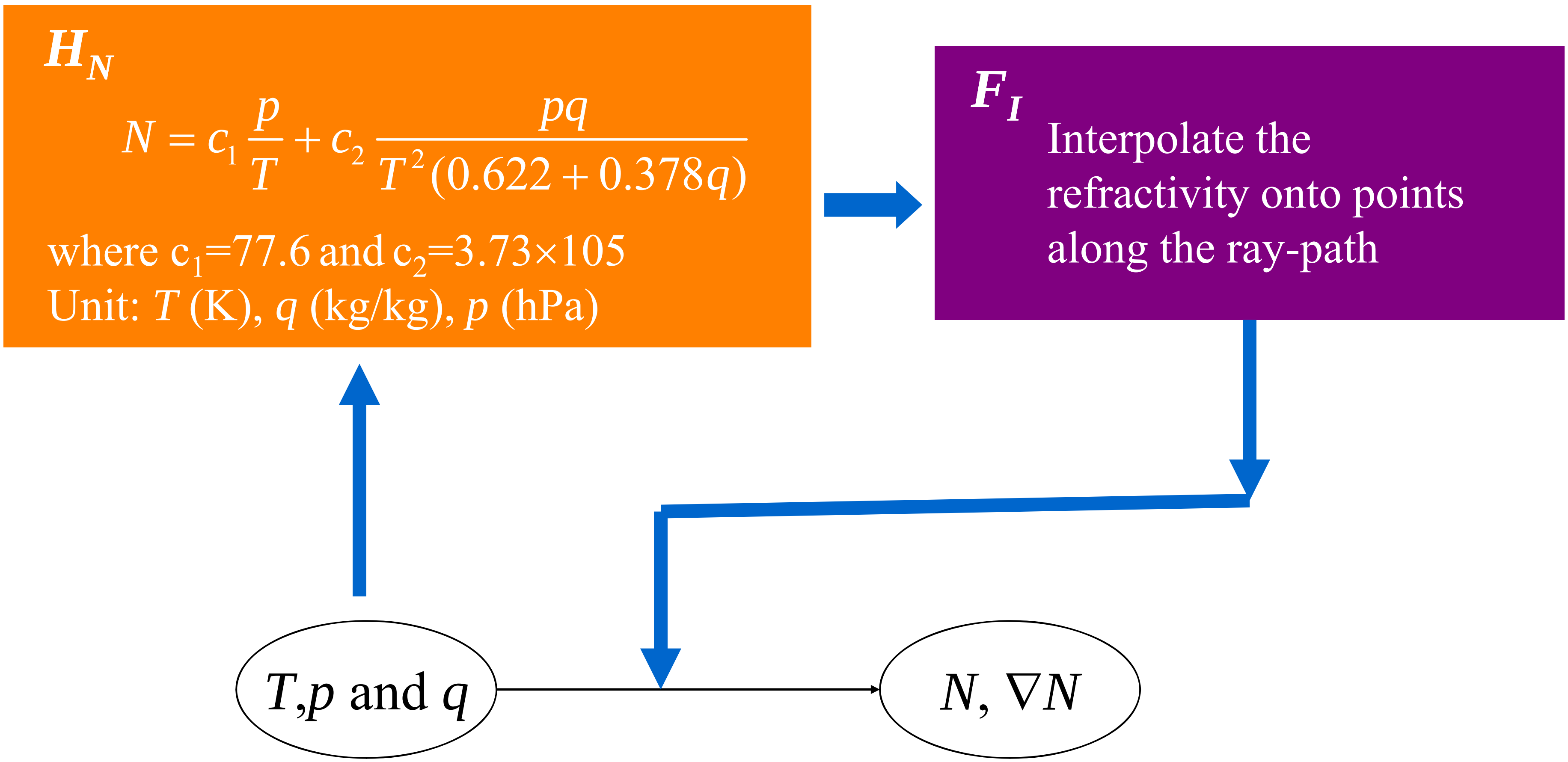

Observation Operator for α

$$\alpha = H_\alpha F_I H_N (T, p, q)$$

H_α

Ray-tracing model: $$\frac{d^2 \vec{x}}{d\tau^2} = n \nabla n$$

where $\vec{x}(\tau)$ is the ray trajectory with $d\tau = ds/n$, s is the length of the ray, and n is the refractivity index.

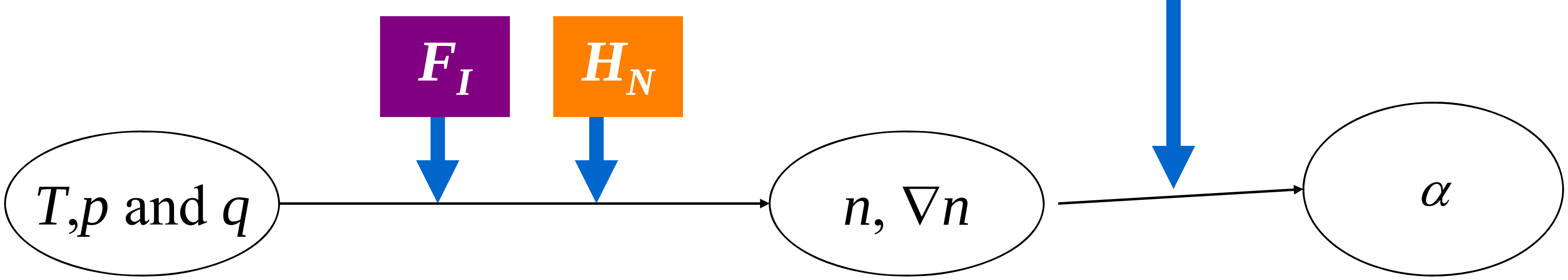

Experiment Design

NOGPS: Control run

BA: Bending angle added to data used in NOGPS

REF: Refractivity added to data used in NOGPS

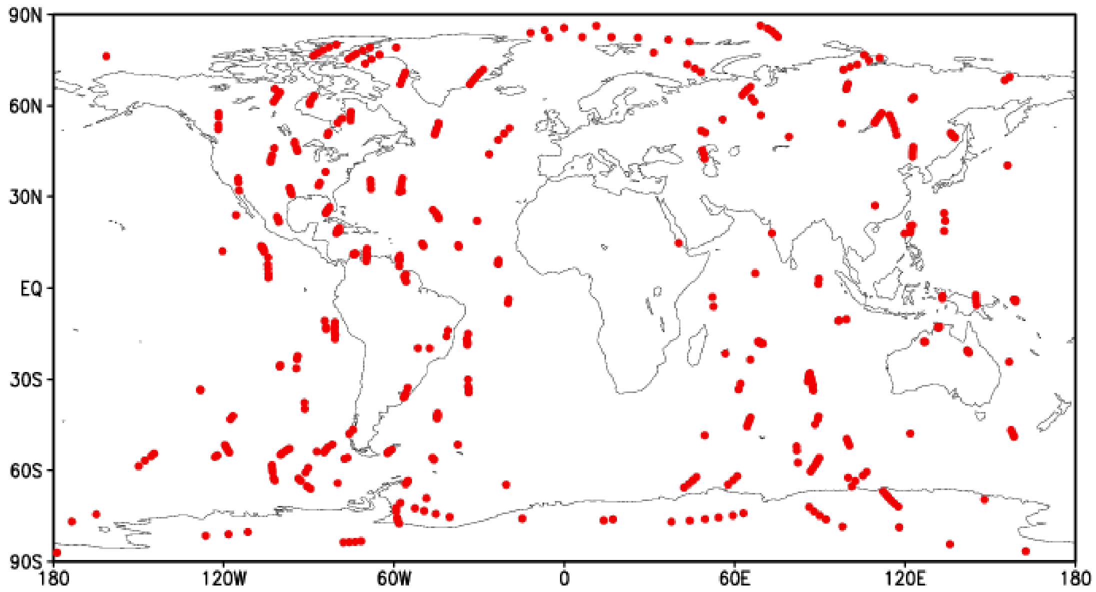

Total 434 ROs

System: NCEP/SSI T170L42

Data: 03-09 UTC from 21-31 May 2002

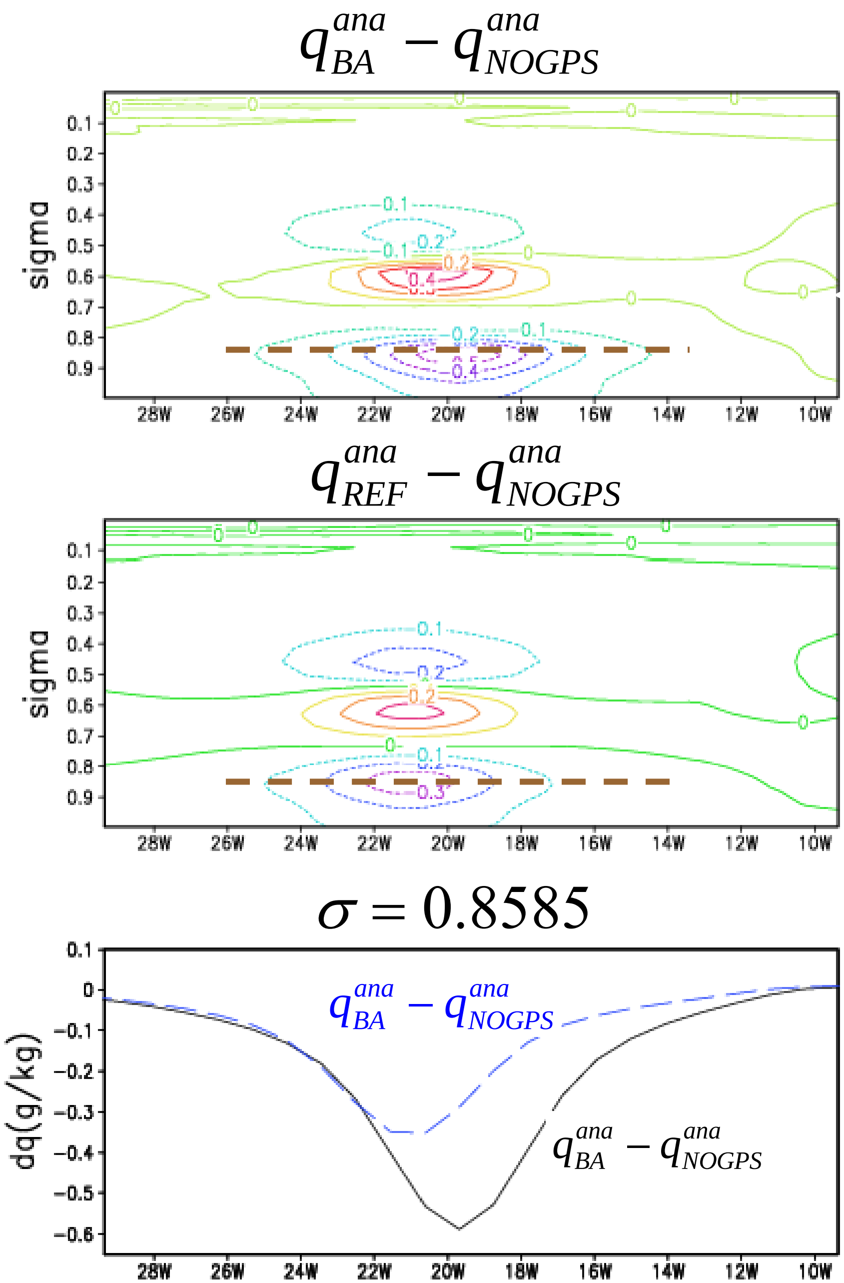

Differences in Moisture Analysis

Cross-section passing through a CHAMP RO observed at 06 UTC 21 May 2002

RO location:

(52.64°N 19.36°W)

Differences in Moisture Analysis (cont.)

Zonal variations averaged over all 434 ROs

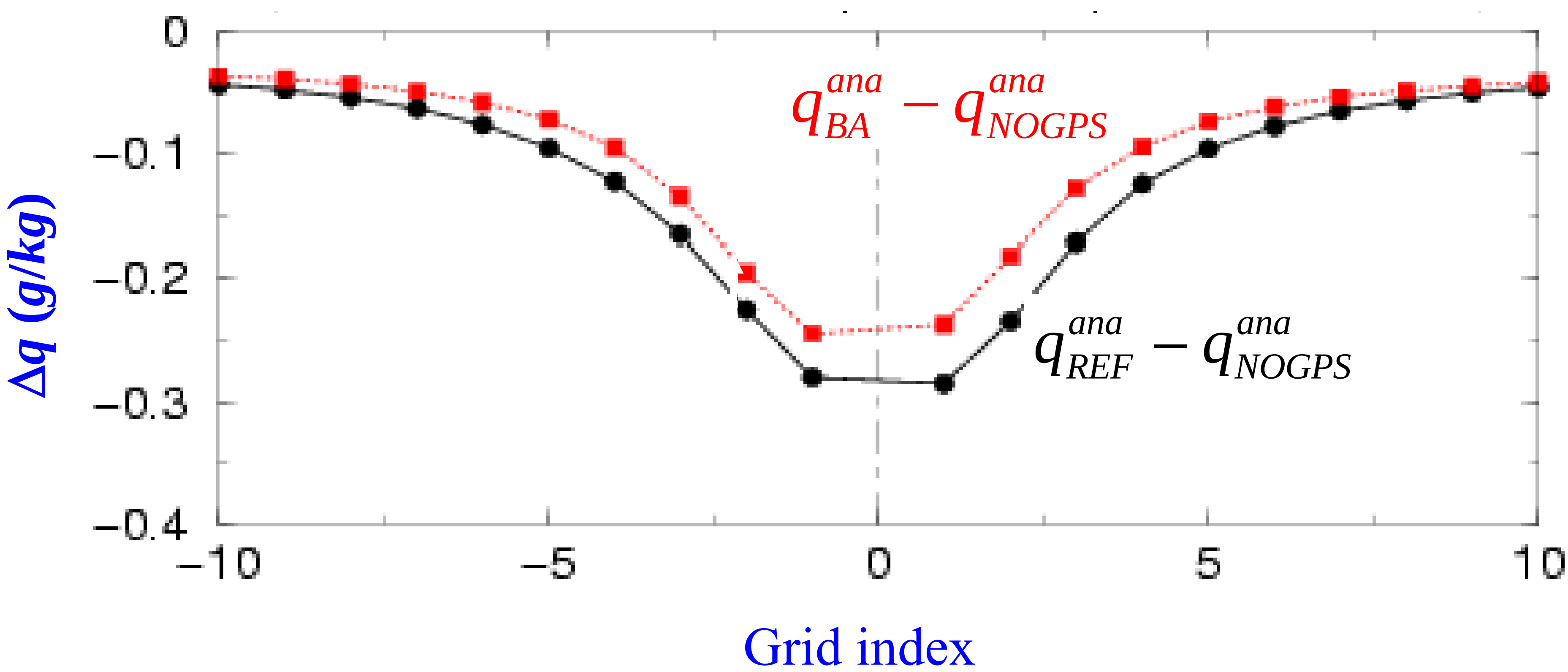

Comparing Three Analyses with CHAMP Refractivity Observations

First, $N^{non\text{-}loc}$ is calculated based on analyses from three data assimilation experiments in the same way as GPS refractivity is derived, i.e., ray-tracing + Abel inversion

Second, calculate the mean and standard deviation of the analysis-modeling refractivity from observations, i.e.,

$$N_{NOGPS}^{non-loc} - N_{CHAMP}^{obs}$$

$$N_{BA}^{non-loc} - N_{CHAMP}^{obs}$$

$$N_{REF}^{non-loc} - N_{CHAMP}^{obs}$$

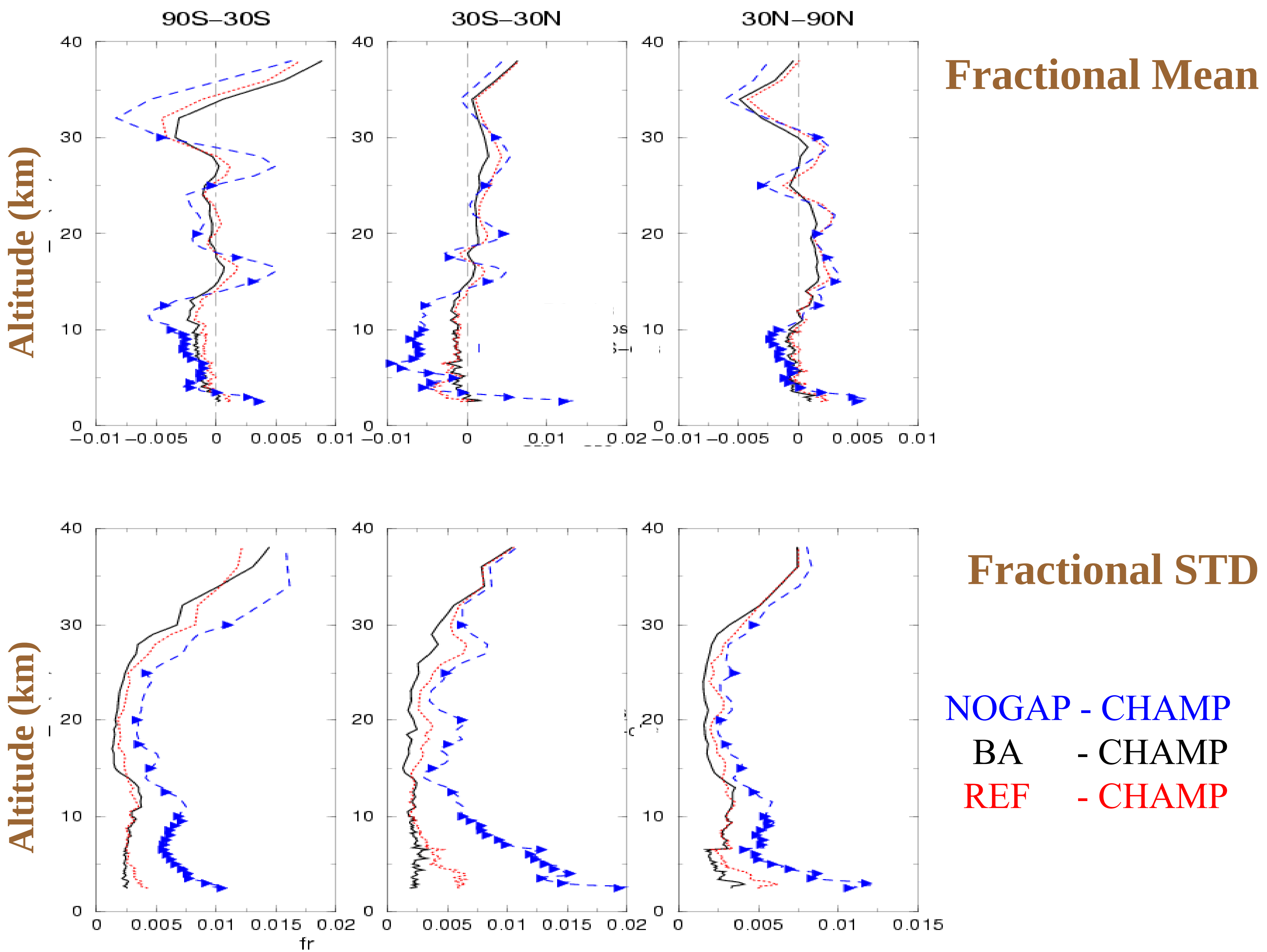
90S–30S
30S–30N
30N–90N
Altitude (km)
Fractional Mean
Fractional STD
NOGAP - CHAMP
BA - CHAMP
REF - CHAMP
fr

(4b) Comparison between local and non-local refractivity assimilation

Schematic Illustration of Non-Local Operator

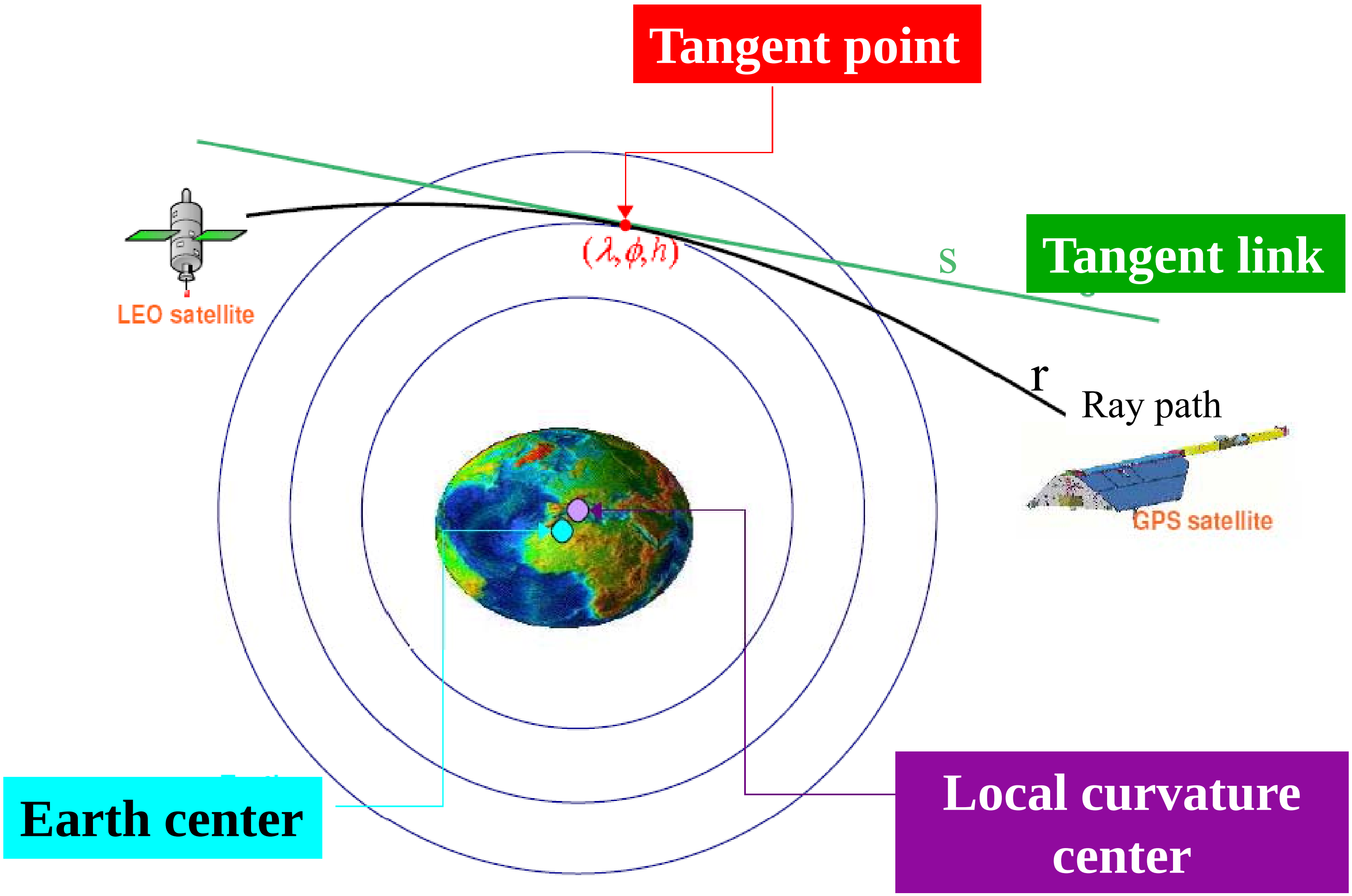

Mathematical Expression of Non-Local Operator

$$\int_r N^{obs} dr = \int_r N^{LOC} dr$$

Approximate the integration along a ray path by its tangent link

$$\int_s N^{obs} ds = \int_s N^{LOC} ds$$

Numerical discretization of the two integrals

$$\mathbf{B} N^{obs} = \mathbf{A} N^{LOC}$$

$$N^{GPS} = \mathbf{K} N^{LOC}$$

$$\mathbf{K} = \mathbf{B}^{-1} \mathbf{A}$$

GPS refractivity (N^{GPS}) is a weighted sum of local refractivity (N^{LOC}) along the tangent link. **K** is the kernel matrix.

An Example of K Distribution

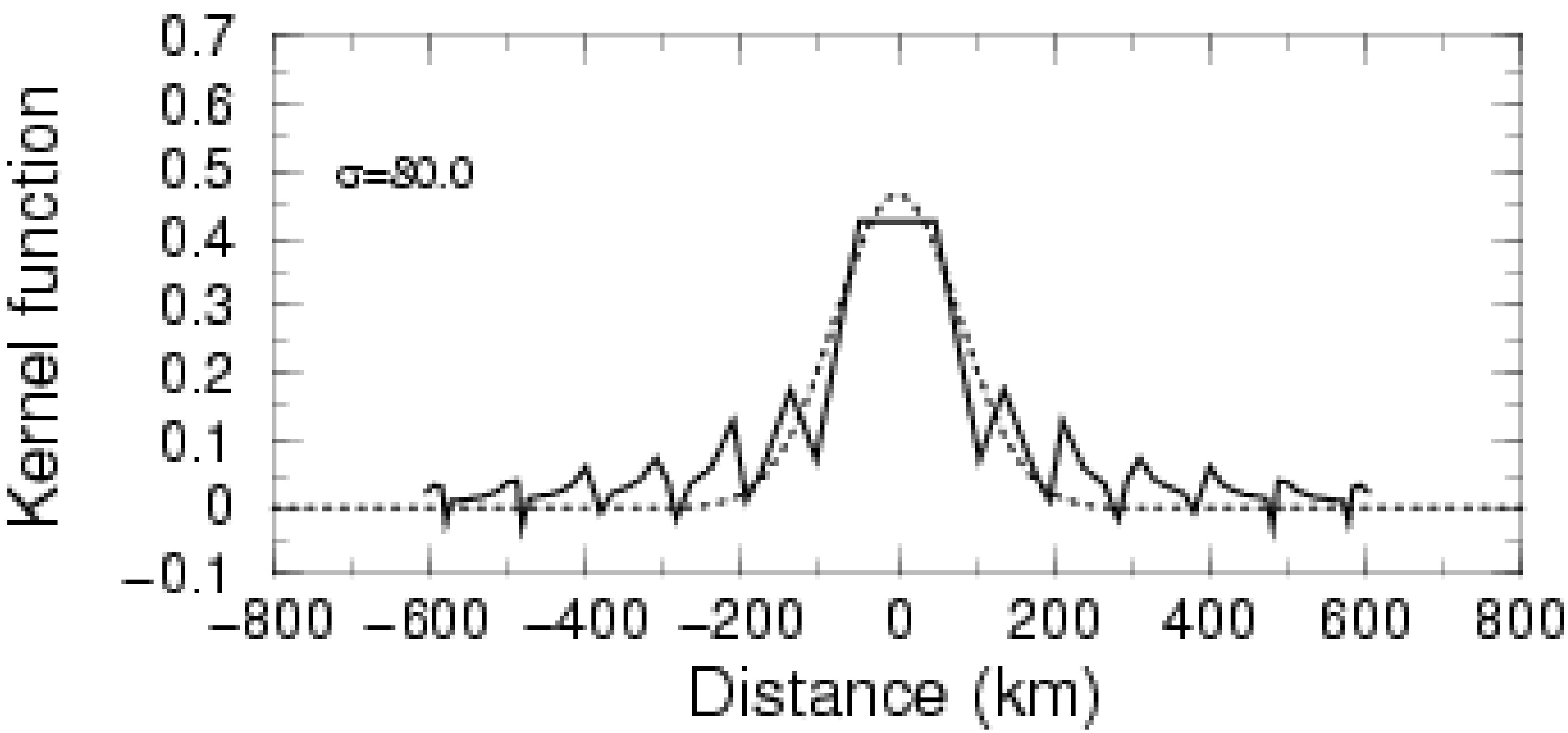

Vertical resolution is 1 *km*. Horizontal resolution is 1°. The tangent link is from west to east. The tangent point is located at (0, 30°N).

Practical Implementation

GPS Observations: $L^{obs} = \mathbf{B}N^{obs}$

Non-local operator: $L = \mathbf{A}N^{LOC}$

$$J = \mathrm{L} + \left(L - L^{obs}\right)^{T} \mathbf{O}^{-1} \left(L - L^{obs}\right)$$

700-hPa Refractivity (contour) and Horizontal Gradients (shaded)

RO1 in large gradient area

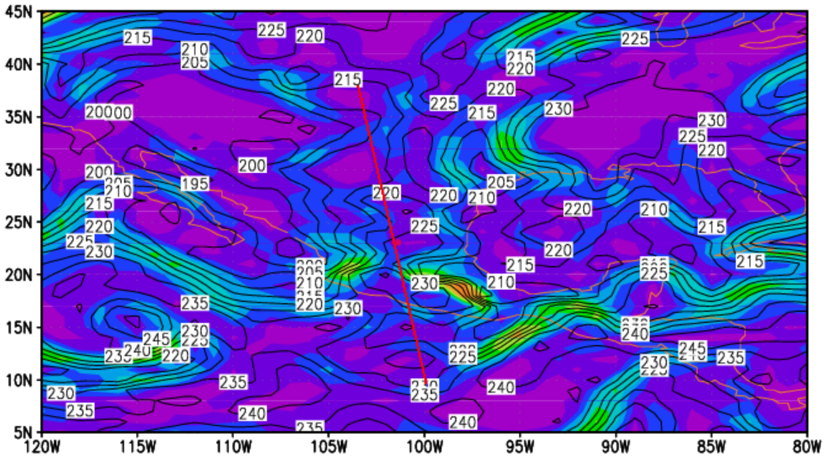

RO2 in small gradient area

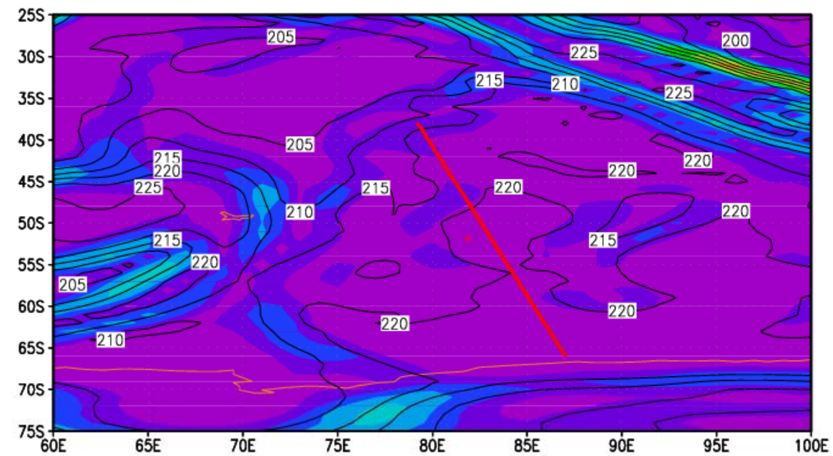

Differences between Model Simulations and GPS CHAMP Observations

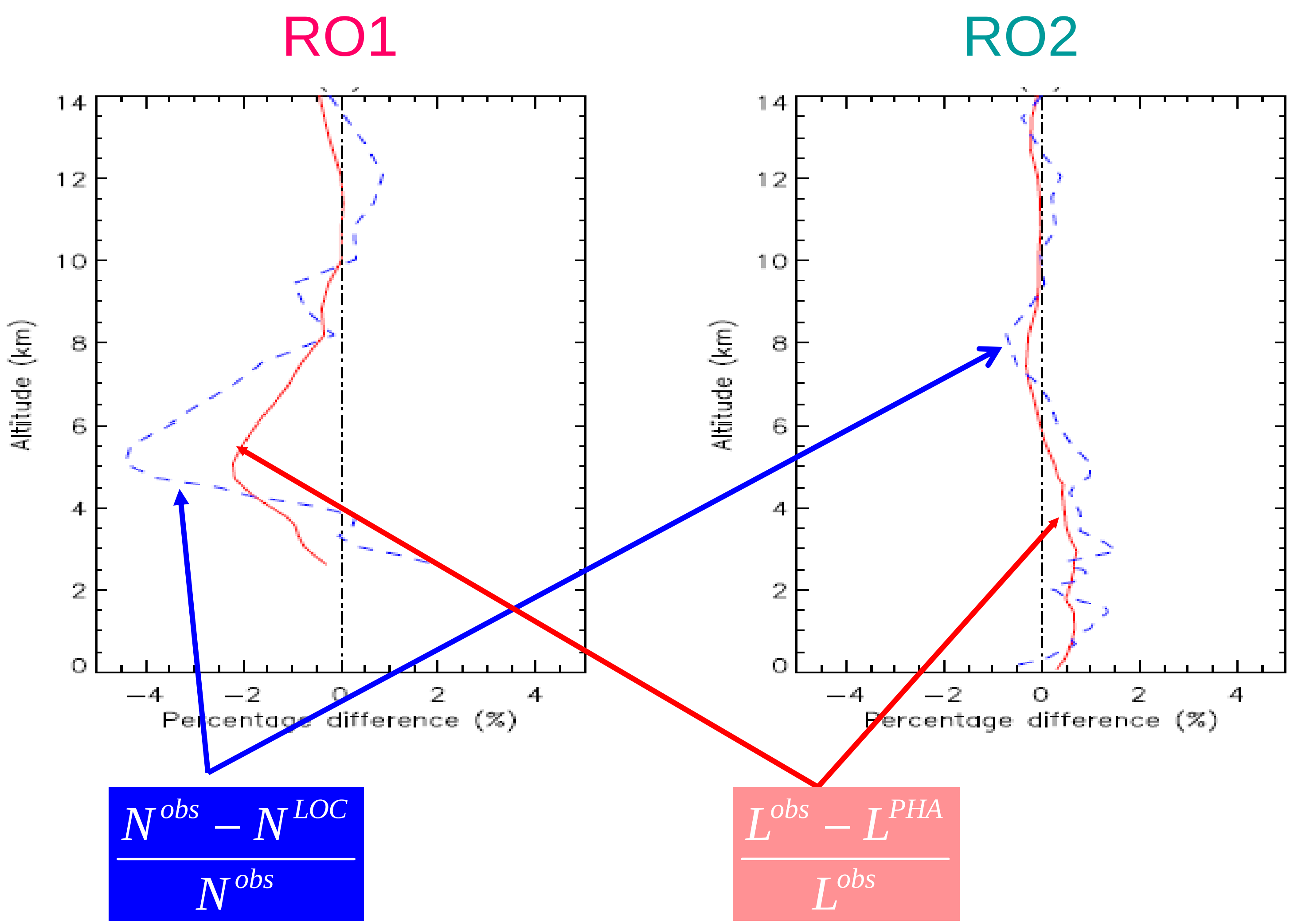

(5) Comparison with Analyses in Cloudy and Clear-Sky Conditions

CloudSat

Instrument: 94-GHz profiling radar

Launch time: April 28, 2006

One orbital time: ~1.5 hours

Along-track resolution: ~1.1 km

Track width: ~1.4 km

Observed variables:
- reflectivity
- liquid/ice water content
- cloud top height
- cloud base height
- cloud types

A CloudSat Orbital Track and a Collocated GPS RO

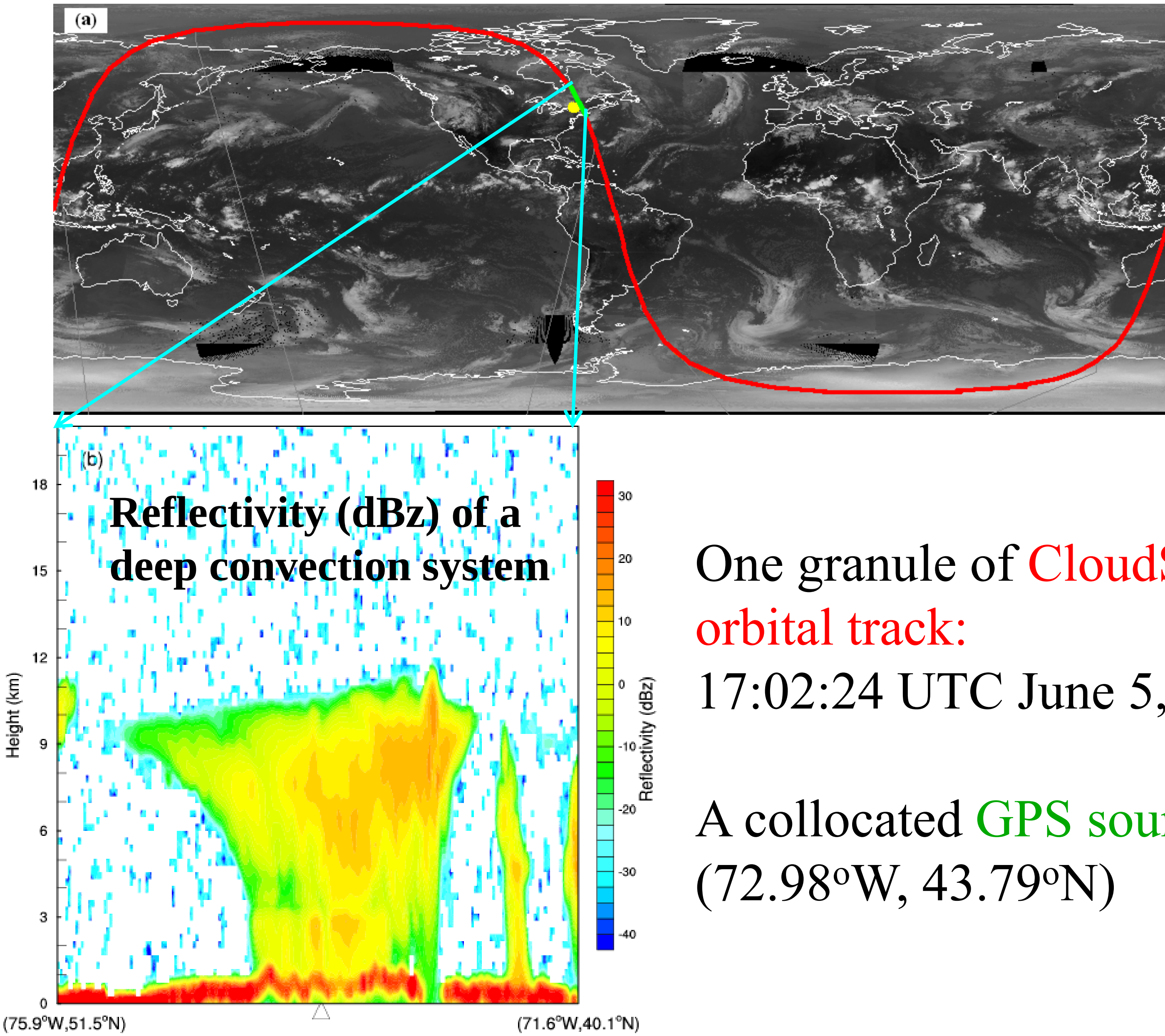

One granule of CloudSat orbital track:
17:02:24 UTC June 5, 2007

A collocated GPS sounding:
(72.98°W, 43.79°N)

Vertical Extent of Different Cloud Types

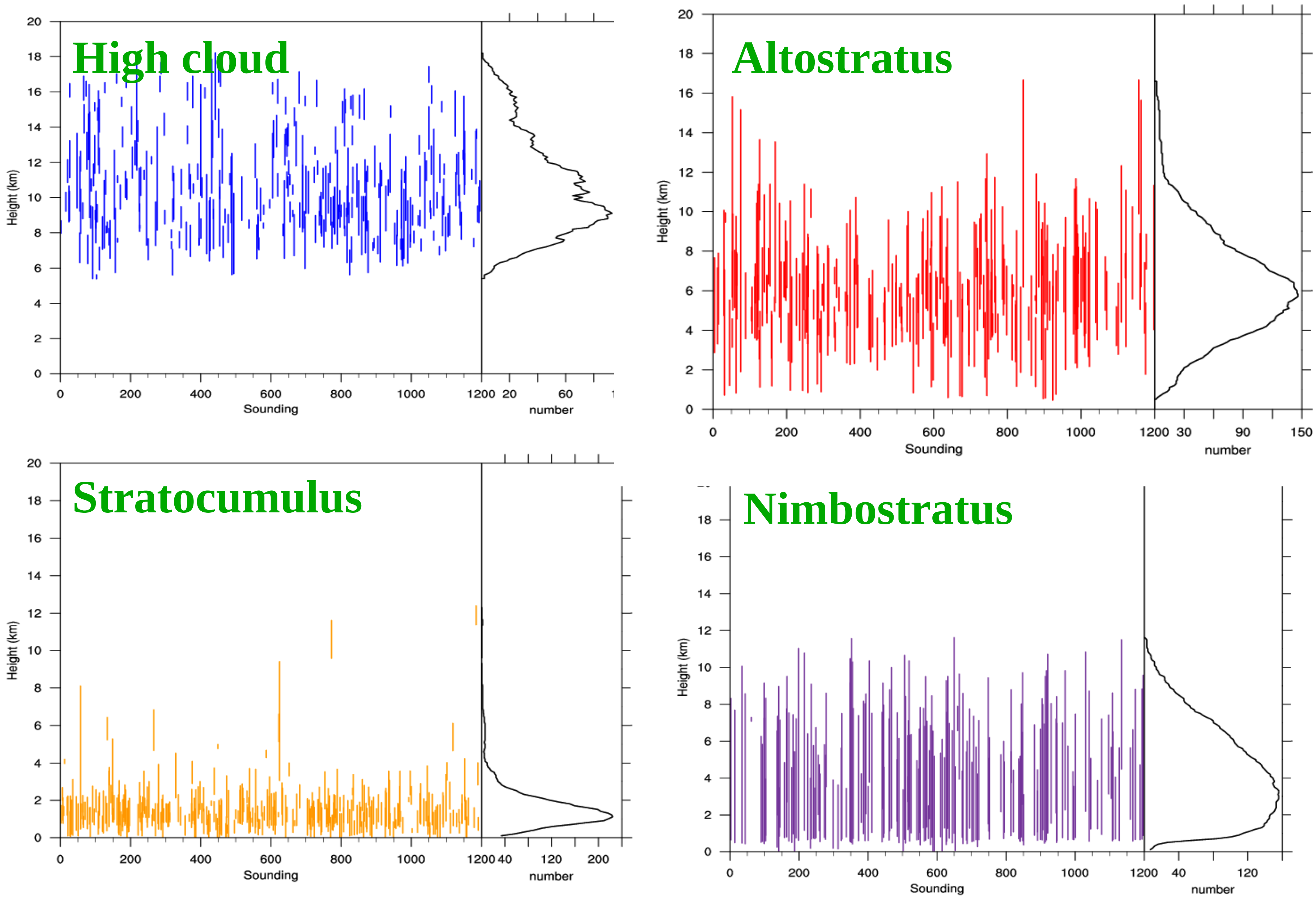

Mean/RMS of Fractional *N* Differences

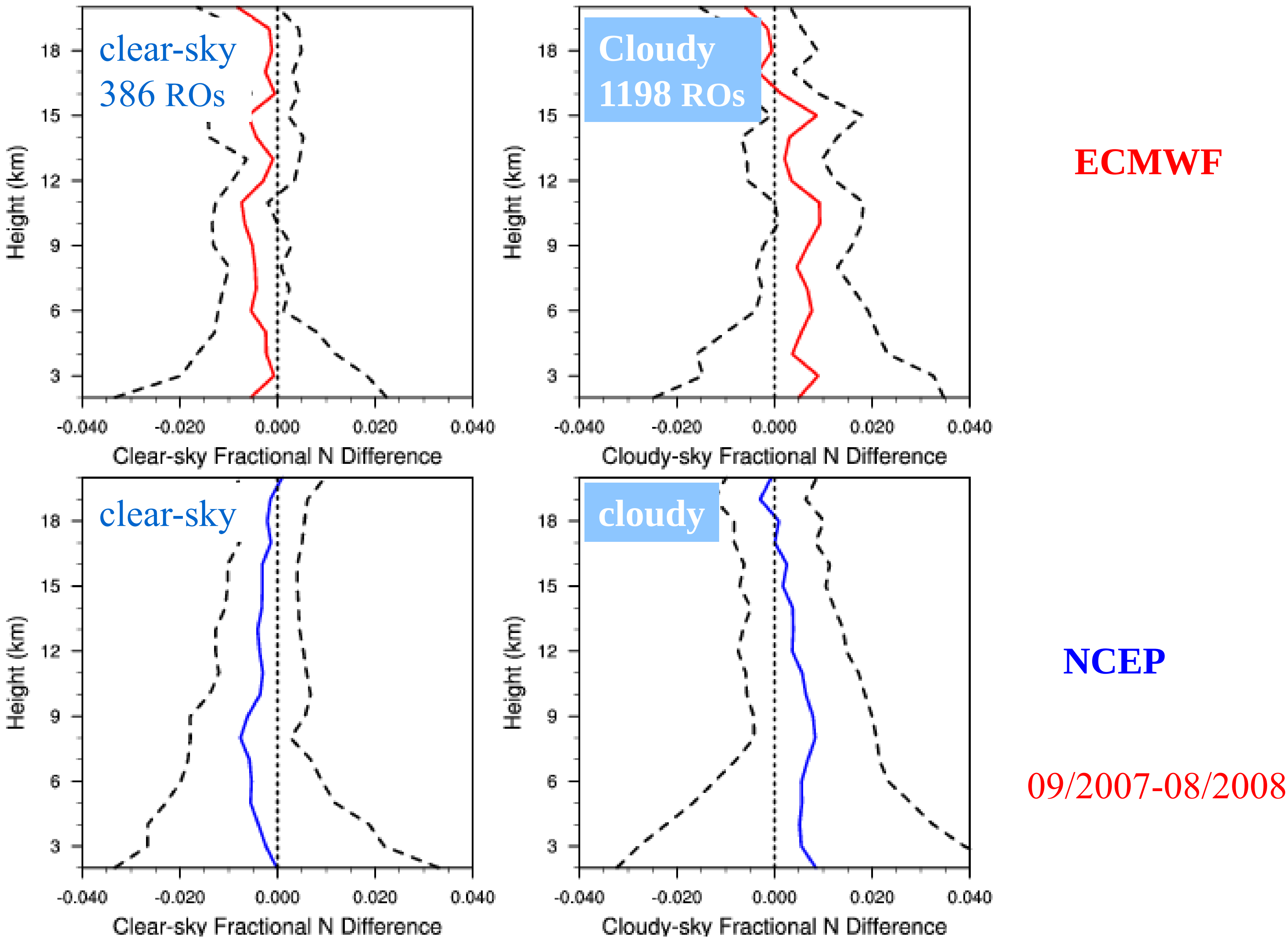

Dependence of Positive *N* Bias on Cloud Type

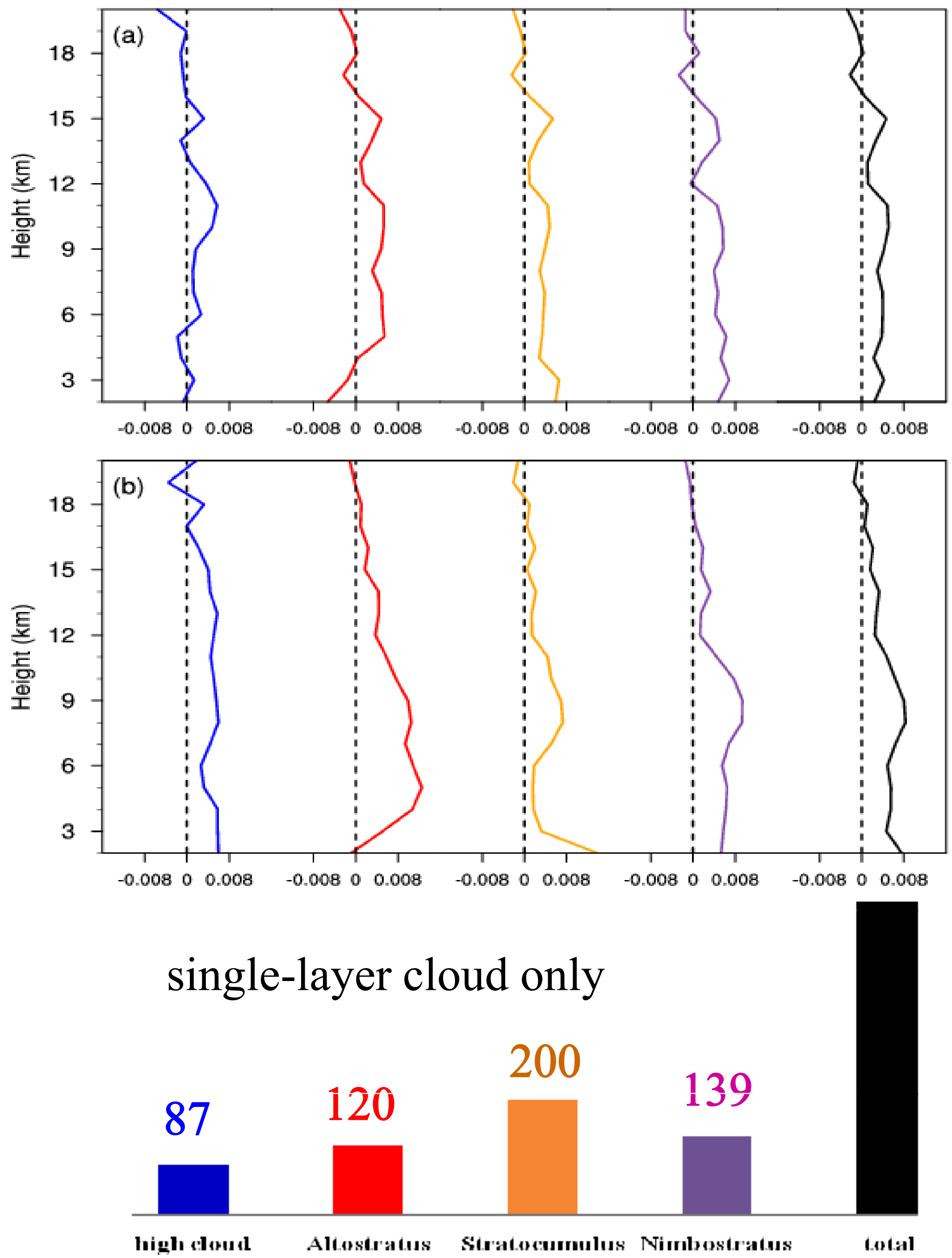

ECMWF

NCEP

High cloud
Altostratus
Stratocumulus
Nimbostratus

(6) Cloudy Retrieval of GPS RO Data

GPS Cloudy Retrieval Algorithm

Assumption: Cloudy air is saturated.

Atmospheric refractivity for cloudy air

GPS observation

$$N = 77.6\frac{P}{T} + 3.73\times 10^5 \frac{e_s(T)}{T^2} + 1.45W = N(T,P)$$

dry term — wet term — liquid water term

Hydrostatic equation:

$$\frac{1}{P}\frac{dP}{dz} = -\frac{g}{R_d T\left(1+0.61q_s\right)}$$

We have two equations for two unknown variables *T* and *P*.

In-cloud profiles of T and p can be uniquely determined from GPS ROs given initial conditions at the cloud top.

Mean Relative Humidity within Clouds

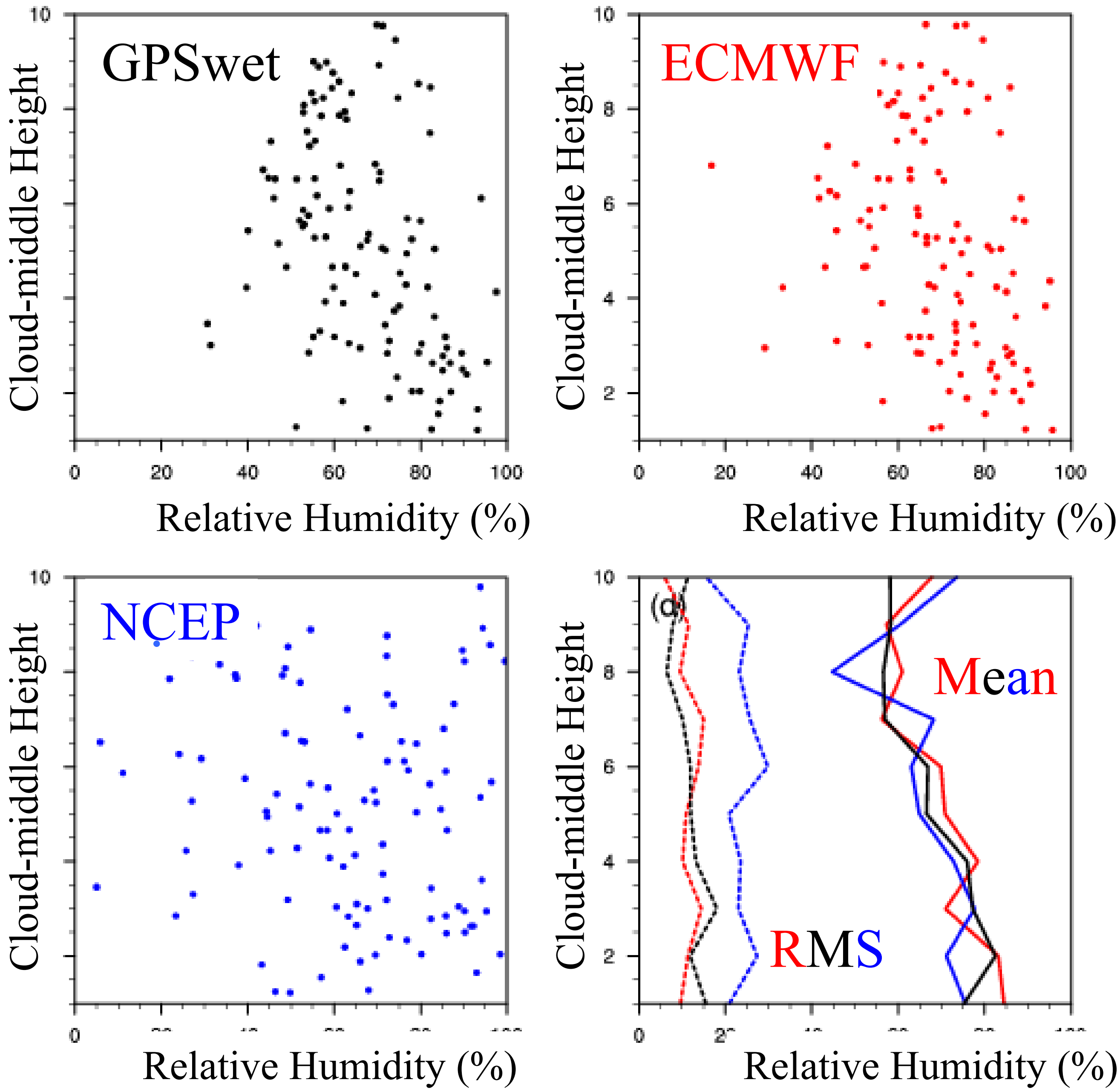

GPS Refractivity within Cloud

Cloud occupies only a fraction of an analysis grid box.

Atmospheric refractivity for cloudy air

$$N^{obs} = N^{dry} + (1-\alpha)\cdot N^{wet} + \alpha \cdot N^{sat}$$

↑ relative humidity parameter

where

$$\alpha = \begin{cases} 5.273 \times IWC + 0.6849, & \text{if } IWC \le 0.05975 gm^{-3} \\ 1, & \text{if } IWC > 0.05975 gm^{-3} \\ 0.85, & \text{for liquid water cloud} \end{cases}$$

Importance of Liquid Water

(with and without including cloud liquid water term)

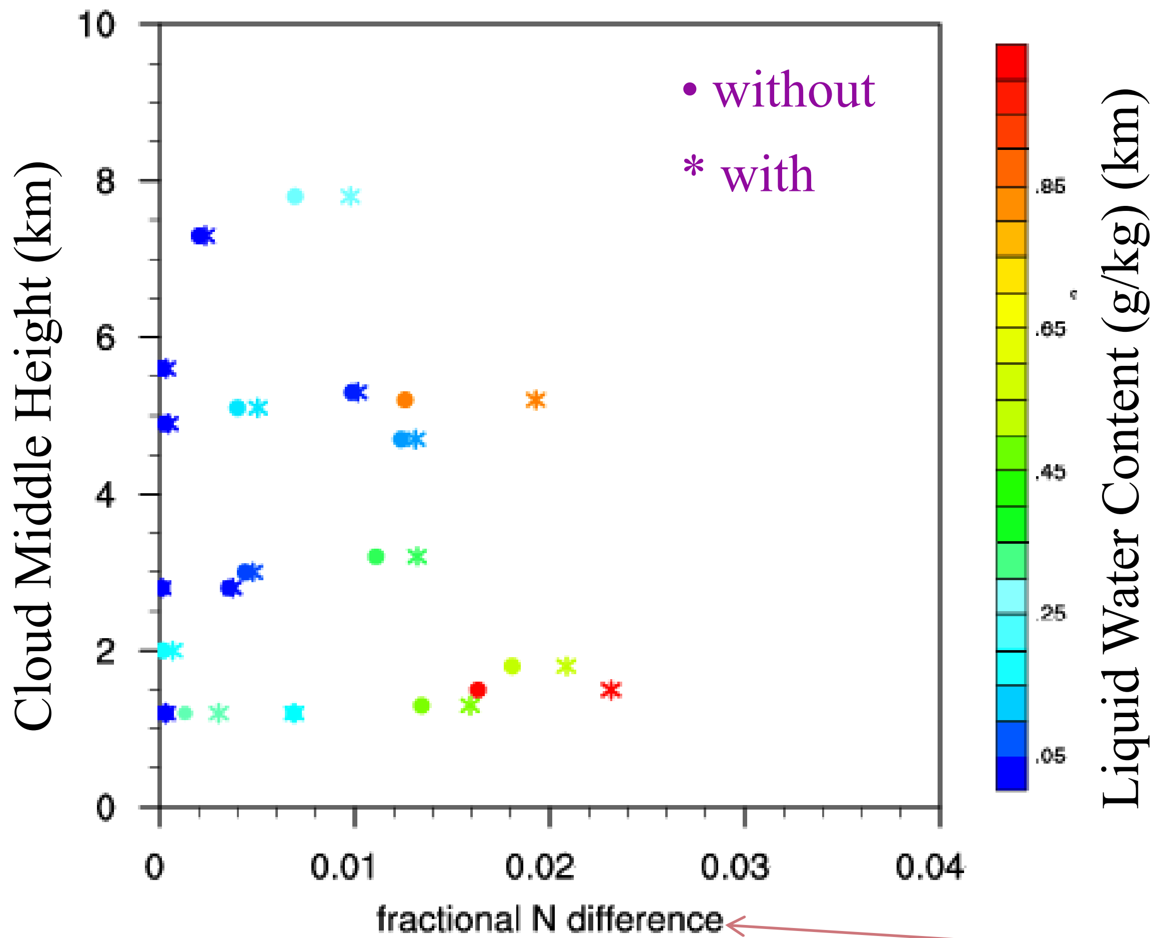

$$\frac{N^{GPS} - N^{ECMWF}}{N^{ECMWF}}$$

(19 water clouds identified by CloudSAT)

Lapse Rates within Cloud

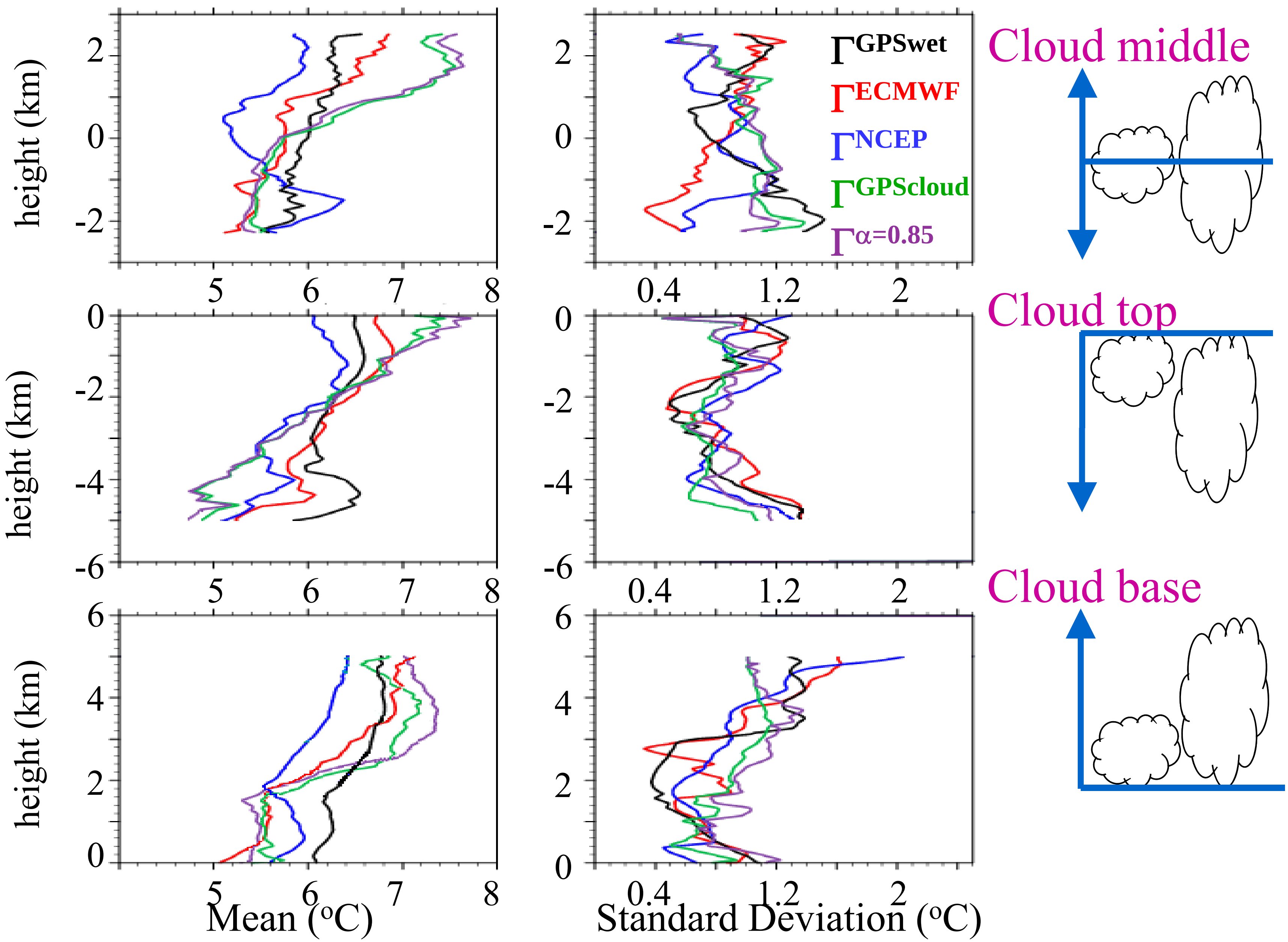

Future Plans

1. **Global cloud climatology derivable from GPS ROs**

2. **Optimal mix of microwave satellite observations with GPS RO data for cloud data assimilation**

3. **Validation of moisture physical parameterization schemes using GPS RO data**

(7) Publications on space-borne GPS RO data assimilation

(1) Zou, X., Y.-H. Kuo, and Y.-R. Guo, 1995: Assimilation of atmospheric radio refractivity using a nonhydrostatic adjoint model. *Mon. Wea. Rev.*, **123**, 2229-2249.

(2) Ware, R., M. Exner, D. Feng, M. Gorbunov, K. Hardy, B. Herman, Y.-H. Kuo, T. Meehan, W. Melbourne, C. Rocken, W. Schreiner, S. Sokolovski, F. Solheim, X. Zou, R. Anthes, and S. Businger, 1996: GPS sounding of the atmosphere from low earth orbit: Preliminary results. *Bull. Am. Meteor.Soc.*, **77**, 19-40.

(3) Rocken, C., R. Anthes, M. Exner, D. Hunt, S. Sokolovskiy, R. Ware, M. Gorbunov, W. Schreiner, D. Feng, B. Herman, Y.-H. Kuo, and X. Zou, 1997: Analysis and validation of GPS/MET data in the neutral atmosphere. *J. Geophys. Res.*, **102**, 29,849-29,866.

(4) Kuo, Y.-H., X. Zou, and W. Huang, 1998: The impact of GPS data on the prediction of an extratropical cyclone: An observing system simulation experiment, *Dyn. Atmos. Ocean.*, **27**, 439-470.

(5) Kuo, Y.-H., X. Zou, S. J. Chen, W. Huang, Y.-R. Guo, R. A. Anthes, M. Exner, D. Hunt, C. Rocken, and S. Sokolovskiy, 1998: A GPS/MET sounding through an intense upper-level front. *Bull. Am. Met. Soc.*, **79**, 617-626.

(7) Publications (cont.)

(6) Zou, X., F. Vandenberghe, B. Wang, M. E. Gorbunov, Y.-H. Kuo, S. Sokolovskiy, J. C. Chang, J. G. Sela, and R. Anthes, 1999: A raytracing operator and its adjoint for the use of GPS/MET refraction angle measurements. *J. Geoph. Res*., **104**, 22,301-22,318.

(7) Zou, X., B. Wang, H. Liu, R. A. Anthes, T. Matsumura, and Y.-J. Zhu, 2000: Use of GPS/MET refraction angles in 3D variational analysis. *Quart. J. Roy. Meteor. Soc*., **126**, 3013-3040.

(8) Liu, H., X. Zou, R. A. Anthes, J. C. Chang, J.-H. Tseng, and B. Wang, 2001: The Impact of 837 GPS/MET bending angle profiles on assimilation and forecasts for the period June 20-30, 1995, *J. Geoph. Res*., **106**, 31771-31786.

(9) Zou, X., H. Liu, and R. A. Anthes, 2002: A statistical estimate of errors in the calculation of radio occultation bending angles caused by a 2D approximation of raytracing and the assumption of spherical symmetry of the atmosphere. *J. Atmos. Oceanic Technol*., **19**, 51-64.

(10) Shao H., and X. Zou, 2002: On the observational weighting and its impact on GPS/MET bending angle assimilation. *J. Geoph. Res*., **107**, ACL 19, 1-28.

(7) Publications (cont.)

(11) Liu, H., and X. Zou, 2003: Improvements to a forward GPS raytracing model and their impacts on assimilation of bending angle, *J. Geoph. Res.*, **108**, D17, 4548.

(12) Zou, X., H. Liu, R. A. Anthes, H. Shao, J. C. Chang, and Y.-J. Zhu, 2004: Impact of CHAMP occultation observations on global analysis and forecasts in the absence of AMSU radiance data. *Journal of the Meteorological Society of Japan*, **82**, 533-549.

(13) Zou, X. and Z. Zeng, 2006: A quality control procedure for GPS RO data. *J. Geoph. Res.*, **111**, D02112, doi:10.1029/2005JD005846.

(14) Zeng, Z and X. Zou, 2006: Application of principle component analysis to CHAMP radio occultation data for quality control and a diagnostic study. *Mon. Wea. Rev.,* **134**, 3263-3282.

(15) Shao, H. and X. Zou, 2009: Test of a non-local excess phase delay operator for GPS RO data assimilation. *J. Applied Remote Sensing,* **3**, 033508, DOI: 10.1117/1.3094060. pp16.

(16) Lin, L., X. Zou, R. Anthes and Y.-H. Kuo, 2010: COSMIC GPS RO temperatures profiles in clouds. *Mon. Wea. Rev*., doi:10.1175/2009MWR2986.1.